

Article

# Effects of Metal Ions on the Flotation of Apatite, Dolomite and Quartz

Yaoyang Ruan , Zeqiang Zhang, Huihua Luo, Chunqiao Xiao, Fang Zhou and Ruan Chi \*

School of Xingfa Mining Engineering, Wuhan Institute of Technology, Wuhan 430074, China; ruanyaoyang@163.com (Y.R.); zzqgxn@hotmail.com (Z.Z.); luohuihua1029@sina.com (H.L.); xcq75@163.com (C.X.); 18995614810@163.com (F.Z.)

\* Correspondence: rac@wit.edu.cn; Tel.: +86-027-8719-5682

Received: 7 March 2018; Accepted: 26 March 2018; Published: 2 April 2018



**Abstract:** The effects of  $\text{Ca}^{2+}$ ,  $\text{Mg}^{2+}$ ,  $\text{Al}^{3+}$ , and  $\text{Fe}^{3+}$  on the flotation behaviors of apatite, dolomite and quartz were investigated through a micro-flotation test, and the influence of calcium ions on the flotation of these minerals was further elucidated by solution chemistry study, zeta potential measurement, and X-ray photoelectron spectroscopy (XPS) analyses. The results indicate that an appropriate amount of  $\text{Ca}^{2+}$  and  $\text{Mg}^{2+}$  can improve the floatability of apatite but had a negligible effect on the flotation performance of dolomite, whereas  $\text{Al}^{3+}$ ,  $\text{Fe}^{3+}$ , and excessive amounts of  $\text{Ca}^{2+}$  decreased the recovery of apatite and dolomite. The studied metal cations can activate quartz at a particular pH. It can be inferred from solution chemistry and zeta potential measurement that the influence of metal ions on the flotation of different minerals should be attributed to the adsorption of various hydrolysis species on the mineral surfaces. XPS analyses reveal that calcium ions can enhance the adsorption of anionic collector on apatite and quartz surfaces, and there are no apparent changes to be observed on the surface of dolomite in the absence and presence of calcium ions at a concentration of  $2.5 \times 10^{-3}$  M, which was in good agreement with the micro-flotation results.

**Keywords:** metal ions; flotation; apatite; dolomite; quartz

## 1. Introduction

Flotation has been widely used for the separation and purification of finely disseminated minerals, and its separation efficiency strongly depends on the selectivity during the flotation process. On the other hand, due to the water quality, dissolution of minerals and consumption of grinding medium, a certain amount of metal ions, such as  $\text{Ca}^{2+}$ ,  $\text{Mg}^{2+}$ ,  $\text{Al}^{3+}$  and  $\text{Fe}^{3+}$ , are inevitably present in the pulp of the actual flotation system [1,2]. Extensive research [2–9] has proven that the floatability of various minerals can be adversely affected by metal ions in the pulp.

Currently, more than 60% of the world's marketable phosphate is upgraded by the flotation process [10]. Fatty acids are commonly used as anionic collectors in phosphate flotation but their use is sensitive to the metal ions [5,11]. Santos et al. [12] reported that calcium and magnesium ions contributed significantly to the decline of apatite recovery and  $\text{P}_2\text{O}_5$  grade. They identified that the metal ions can react with fatty acid, resulting in reagent consumption. Al-Thyabat and Al-Zoubi [13] pointed out that the presence of  $\text{Ca}^{2+}$  and  $\text{Mg}^{2+}$  in water was detrimental to phosphate flotation. It was explained that the collector would react with free divalent metal ions in the pulp to form metal carboxylate complexes or precipitates on both quartz and phosphate instead of selectively reacting to the calcium sites on the surface of phosphate particles. Elgillani and Abuozaid [14] claimed that the dissolved  $\text{Ca}^{2+}$  in the system should be responsible for the reduction of apatite depression by its effect on the stabilization of apatite, causing the removal of carbonates from phosphate minerals to be less

efficient. Sis and Chander [11] observed the detrimental effect of  $\text{Ca}^{2+}$  on the hydrophobicity of apatite by contact angle measurement, as the contact angle decreased with the increase of  $\text{Ca}^{2+}$  concentration.

However, the majority of previous research was focused on the treatment of actual phosphate ore in the presence of divalent calcium and magnesium ions, and the mechanism of the detrimental effects of metal ions, including  $\text{Al}^{3+}$  and  $\text{Fe}^{3+}$ , still remains to be determined. Moreover, it is well-known that apatite is the main valuable mineral in actual phosphate ore while the major carbonate and silicate gangue minerals are dolomite and quartz, respectively [15]. Therefore, to further understand the effects and mechanism of metal ions on the flotation of the phosphate ore, it was necessary to first explore the effects of metal ions on the flotation behaviors of apatite, dolomite, and quartz, separately.

The effects of  $\text{Ca}^{2+}$ ,  $\text{Mg}^{2+}$ ,  $\text{Al}^{3+}$ , and  $\text{Fe}^{3+}$  on the flotation of apatite, dolomite, and quartz were systemically investigated by micro-flotation tests. Based on the solution equilibrium constants, the distribution diagrams for the hydrolysis species of polyvalent metal ions at the initial concentration of  $2.5 \times 10^{-3}$  M were obtained, in order to interpret the different flotation behaviors of various minerals caused by metal ions in aqueous solution. Furthermore, the adsorption mechanisms of hydrolysis species of  $\text{Ca}^{2+}$  on apatite, dolomite, and quartz were evaluated by zeta potential measurement and X-ray photoelectron spectroscopy (XPS).

## 2. Materials and Methods

### 2.1. Pure Minerals

The crystal apatite was sorted from Madagascar in South Africa while the pure quartz and dolomite samples were taken from Hubei province in China. The mineral purities were examined by X-ray diffraction (XRD) analysis and the results (seen in Figure 1) indicated that the phosphate mineral occurred in the form of fluorapatite and that there were no other minerals detected other than the three pure minerals. Prior to the batch flotation experiments, the samples were successively subjected to hammer crushing and grinding with an agate mortar. The samples were sieved to obtain the fractions of  $-0.074$  mm and  $-0.038$  mm, which were used for micro-flotation tests and zeta potential measurements, respectively.

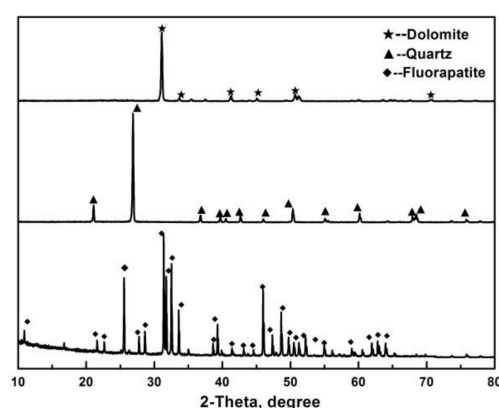


Figure 1. The XRD patterns of apatite, dolomite, and quartz.

### 2.2. Reagents

Cottonseed oil bought from the local market was chosen as an anionic collector for the flotation experiment after being saponified by sodium hydroxide [16]. Analytical grade calcium chloride, aluminium chloride, magnesium chloride hexahydrate, and ferric chloride hexahydrate were purchased from Sinopharm Chemical Reagent Co., Ltd., Ningbo, China. These chemical compounds were used to generate various metal ions in aqueous solution with the objective of investigating their effects on the flotation of apatite, dolomite, and quartz. Hydrochloric acid and sodium hydroxide

solution, at a concentration of 10%, were used for pH adjustment, and distilled water was used throughout the experiments.

### 2.3. Micro-Flotation Test

The flotation test was conducted in a laboratory flotation machine with a 50 mL cell and the concentration of cottonseed oil soap was fixed at 60 mg/L ( $2.14 \times 10^{-4}$  M). Precisely 2.00 g of pure mineral was conditioned for 5 min in the cell with 50 mL aqueous solution at a determined pH and metal ion concentration. The pulp was aerated with a flowrate of 0.1 L/min, and the sample was floated for 5 min with impeller speed of 2000 rpm. Subsequently, the froth product was filtered, dried, and weighed to calculate the recovery.

### 2.4. Zeta Potential Measurement

The electrophoretic measurements were performed by a zeta potential analyzer (Zetasizer Nano-ZS90, Malvern, UK). Fifty milligrams of the  $-0.038$  mm fraction sample was suspended in 100 mL solution at the determined pH and calcium ion concentration ( $2.5 \times 10^{-4}$  M and  $2.5 \times 10^{-3}$  M). The mineral particles were dispersed for 10 min by ultrasonic agitation at room temperature. The final pH of the solution was measured and recorded. Subsequently, the suspension was centrifuged and the supernatant was taken for zeta potential measurements. Each measurement was repeated three times to provide an average value.

### 2.5. X-ray Photoelectron Spectroscopy (XPS) Analyses

Samples and the float products with 60 mg/L cottonseed oil soap in the absence and presence of  $2.5 \times 10^{-3}$  M  $\text{Ca}^{2+}$  were collected and dried at ambient temperature. The XPS analyses were carried out with a Thermo Scientific (Waltham, MA, USA) ESCALAB 250Xi spectrometer using a monochromatic Al K $\alpha$  source ( $h\nu = 1486.8$  eV). The pressure of the analyzer chamber was less than  $2 \times 10^{-9}$  Torr. High-resolution spectra were obtained with a pass energy of 30 eV. The binding energy of C1s at 284.8 eV was used to calibrate the spectrometer. Spectra were analyzed using XPS Peak software (version 4.1, Hongkong, China), and the lines were fitted with a Gaussian–Lorentzian product function after Shirley background subtraction. The Gaussian–Lorentzian mix ratio was taken as 20% for all lines.

## 3. Results and Discussion

### 3.1. Flotation Behavior of Pure Minerals in the Presence of Metal Ions

The effect of pH and ionic concentration on the floatability of apatite in the presence of different metal ions is shown in Figure 2. It can be seen from Figure 2a that apatite recovery in the absence of metal ions dramatically increased with increasing pH values (4.5–8.0), and then decreased as the pH continuously increased. The maximum recovery of 78.27% was achieved at pH around 8.0  $\text{Ca}^{2+}$ , and  $\text{Mg}^{2+}$  exhibited a beneficial effect on the floatability of apatite as the recovery in the presence of  $\text{Ca}^{2+}$  and  $\text{Mg}^{2+}$  was higher than that without metal ions.  $\text{Al}^{3+}$  and  $\text{Fe}^{3+}$  were proved unfavorable to the flotation of apatite, especially for  $\text{Fe}^{3+}$  since the apatite recovery was less than 10% over the entire pH range.

Figure 2b further demonstrates the effect of the concentration of various metal ions on the flotation performance of apatite at neutral pH. It was clear that a proper concentration of  $\text{Ca}^{2+}$  in solution can promote the recovery, which was in accordance with the findings of Horta et al. [17]. Another similar result was reported by Tohry and Dehghani when they investigated the influence of  $\text{Ca}^{2+}$  on the reduction of apatite content for the beneficiation of a siliceous-phosphorus iron ore [18]. The beneficial effect caused by  $\text{Mg}^{2+}$  was observed for the entire concentration range, as the curve of  $\text{Mg}^{2+}$  was above the baseline (i.e., no metal ions). Increasing the  $\text{Al}^{3+}$  concentration resulted in a steady decline in apatite recovery. The presence of  $\text{Fe}^{3+}$  sharply reduced the floatability of apatite above concentrations of  $10^{-5}$  M to  $10^{-4}$  M and little recovery was observed when the concentration was more than  $5 \times 10^{-3}$  M.

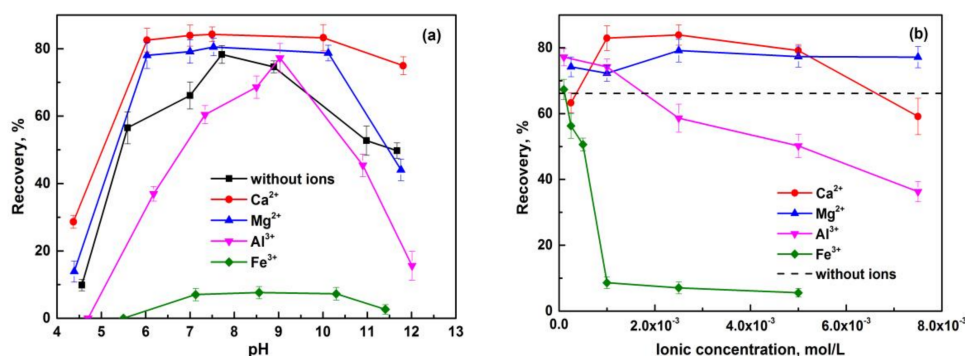


**Figure 2.** (a) Effect of pH on the floatability of apatite in the presence of metal ions at a concentration of  $2.5 \times 10^{-3}$  M; (b) Effect of ionic concentration on the floatability of apatite at neutral pH.

The flotation results of dolomite in the presence of metal ions are plotted in Figure 3. It was found that the floatability of dolomite was excellent in distilled water, as the recovery rate was around 80% over the entire range of pH (5.9–11.3).  $\text{Ca}^{2+}$  and  $\text{Mg}^{2+}$  had a marginal effect on the flotation performance of dolomite until the pH of the solution changed from 10 to 11, which agrees with the results reported by Zhang et al. [19]. The floatability of dolomite was affected by  $\text{Al}^{3+}$  and  $\text{Fe}^{3+}$ , especially in the pH range 6.0–7.0. It is evident that  $\text{Al}^{3+}$  and  $\text{Fe}^{3+}$  have a depression effect on the flotation of dolomite, but the depression reduced as the pH increased.

The results given in Figure 3b clearly depict the depression effect of metal ions on dolomite flotation as a function of concentration at neutral pH.  $\text{Ca}^{2+}$  and  $\text{Mg}^{2+}$  had a negligible effect on dolomite flotation when the concentration was no more than  $2.5 \times 10^{-3}$  M, but exhibited a detrimental effect when the concentration exceeded  $5 \times 10^{-3}$  M.  $\text{Al}^{3+}$  and  $\text{Fe}^{3+}$  would strongly depress the flotation of dolomite even at a low concentration. The depression effect caused by these metal ions could be attributed to reaction of cations with fatty acid into precipitation, decreasing the concentration of the collector available for adsorption onto the dolomite surfaces [20].

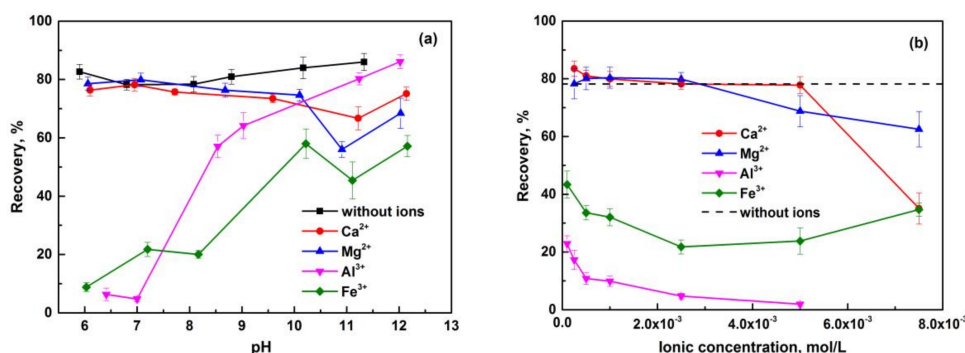


**Figure 3.** (a) Effect of pH on the floatability of dolomite in the presence of metal ions at a concentration of  $2.5 \times 10^{-3}$  M; (b) Effect of ionic concentration on the floatability of dolomite at neutral pH.

Pure quartz cannot be floated without being activated using anionic collectors, such as fatty acids. Figure 4 presents the flotation results of quartz after activation by various metal ions. For  $\text{Mg}^{2+}$ ,  $\text{Al}^{3+}$  and  $\text{Fe}^{3+}$  as activators, the recovery of quartz increased to maximum at pH 9–10 then decreased with increasing pH. Quartz started to float at pH of 9.0 and a sharp improvement of recovery was observed from 9.5 to 11.5 in the presence of  $\text{Ca}^{2+}$ , which was in agreement with the adsorption of calcium species on quartz surfaces reported by Ananthapadmanabhan and Somasundaran [21]. Moreover, it is evident from Figure 4a that the activation abilities caused by metal ions can be determined in the order of  $\text{Ca}^{2+} \geq \text{Mg}^{2+} > \text{Fe}^{3+} > \text{Al}^{3+}$ .

The concentration of various metal ions significantly affected the flotation behavior of quartz as well. Figure 4b shows that quartz recovery increased as the ion concentration increased, and then decreased with the further increase of concentration. Therefore, it can be concluded that the favorable condition was  $\text{Ca}^{2+}$  and  $\text{Fe}^{3+}$  at a concentration of  $2.5 \times 10^{-3}$  M, whereas the concentration was  $10^{-3}$  M for  $\text{Mg}^{2+}$  and  $\text{Al}^{3+}$  under the desired pH for activation.

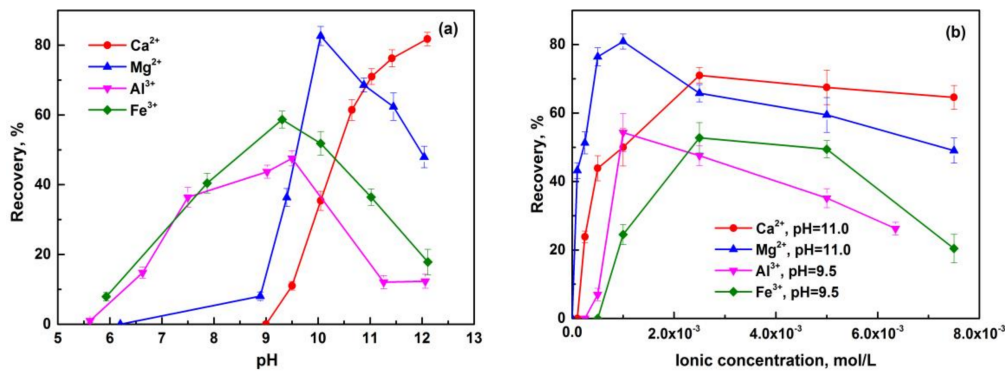


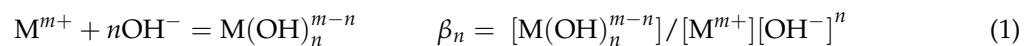
**Figure 4.** (a) Effect of pH on the floatability of quartz in the presence of metal ions at a concentration of  $2.5 \times 10^{-3}$  M; (b) Effect of ionic concentration on the floatability of quartz at the desired pH.

On the basis of the results and discussion above, metal ions affected the floatability of apatite and dolomite similarly, suggesting that their flotation selectivity would be poor at moderate metal ion concentration in neutral and alkaline conditions. Meanwhile, unintentional activation of quartz by metal ions would result in phosphate grade reduction. Thus, it is necessary to reduce the pulp metal ion concentration when beneficiating the phosphate ore by flotation.

### 3.2. Hydrolysis Equilibria of Metal Ions

The flotation behavior of apatite, dolomite, and quartz varies with the change of pH in the absence and presence of metal ions, thus the hydrolysis species are thought to be responsible for the different flotation behaviors. To interpret the influence of polyvalent metal ions on the flotation behavior of apatite, dolomite, and quartz, the concentration of each hydrolysis component was calculated based on the solution equilibria of the cations. Distribution diagrams for  $2.5 \times 10^{-3}$  M  $\text{Ca}^{2+}$ ,  $\text{Mg}^{2+}$ ,  $\text{Al}^{3+}$ , and  $\text{Fe}^{3+}$  as a function of pH were obtained to evaluate the interactions between the mineral surface and hydrolysis species.

In homogeneous systems, the hydrolysis of polyvalent metal ions is shown below [22].



Thus,

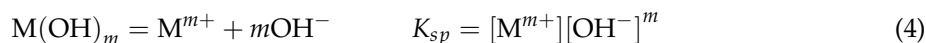
$$[\text{M}] = \frac{[\text{M}^{m+}] + [\text{MOH}^{m-1}] + [\text{M}(\text{OH})_2^{m-2}] + \dots + [\text{M}(\text{OH})_n^{m-n}]}{1 + \beta_1[\text{OH}^-] + \beta_2[\text{OH}^-]^2 + \dots + \beta_n[\text{OH}^-]^n} \quad (2)$$

where  $\beta_1, \beta_2, \dots, \beta_n$ , are cumulative stability constants,  $[\text{M}]$  represents the initial concentration of metal ions in solution.

The concentration of free metal ions is given by

$$\log [\text{M}^{m+}] = \log [\text{M}] - \log (1 + \beta_1[\text{OH}^-] + \beta_2[\text{OH}^-]^2 + \dots + \beta_n[\text{OH}^-]^n) \quad (3)$$

When metal ions start to precipitate in solutions, the concentration of free metal ions can be calculated by:



$$\log [M^{m+}] = \log K_{sp} - m \log [OH^-] \quad (5)$$

The concentration of other species can be obtained by Equation (1),

$$\log [M(OH)_n^{m-n}] = \log \beta_n + \log [M^{m+}] + n \log [OH^-] \quad (6)$$

With reference to Equations (3), (5) and (6), and the relevant stability constants shown in Table 1, the concentration of hydrolysis species of  $Ca^{2+}$ ,  $Mg^{2+}$ ,  $Al^{3+}$ , and  $Fe^{3+}$  was calculated and the species distribution diagrams of various metal ions as a function of pH at the ionic strength of  $2.5 \times 10^{-3}$  M can be plotted (Figure 5).

**Table 1.** The stability constants of the metallic ionic hydroxyl complex.

Metal Ions	Stability Constants				$pK_{sp}, M(OH)_m$
	$\log\beta_1$	$\log\beta_2$	$\log\beta_3$	$\log\beta_4$	
$Ca^{2+}$	1.40	2.77	/	/	5.22
$Mg^{2+}$	2.58	1.00	/	/	11.15
$Al^{3+}$	9.01	18.70	27.00	33.00	33.50
$Fe^{3+}$	11.81	22.30	32.05	34.30	38.80

As shown in Figure 5, it can be seen that  $Mg^{2+}$  and  $Fe^{3+}$  begin to precipitate when the pH is up to 9.8 and 2.1, respectively.  $Al(OH)_3$  precipitation is the dominant species in the pH range 3.8–11.8, whereas  $Ca(OH)_2$  precipitation does not exist in an aqueous solution over the entire pH range. Therefore,  $Al^{3+}$  and  $Fe^{3+}$  were in the form of insoluble metal hydroxide throughout the pH range of micro-flotation tests.  $Al(OH)_3$  and  $Fe(OH)_3$  could preferentially precipitate on the mineral surface [23], and the hydrophilicity of apatite and dolomite was enhanced, resulting in the reduction of the adhesion of surfactant molecules on the mineral surface. That is why the floatability of apatite and dolomite decreased in the presence of  $Al^{3+}$  and  $Fe^{3+}$ , as shown in Figures 2 and 3.

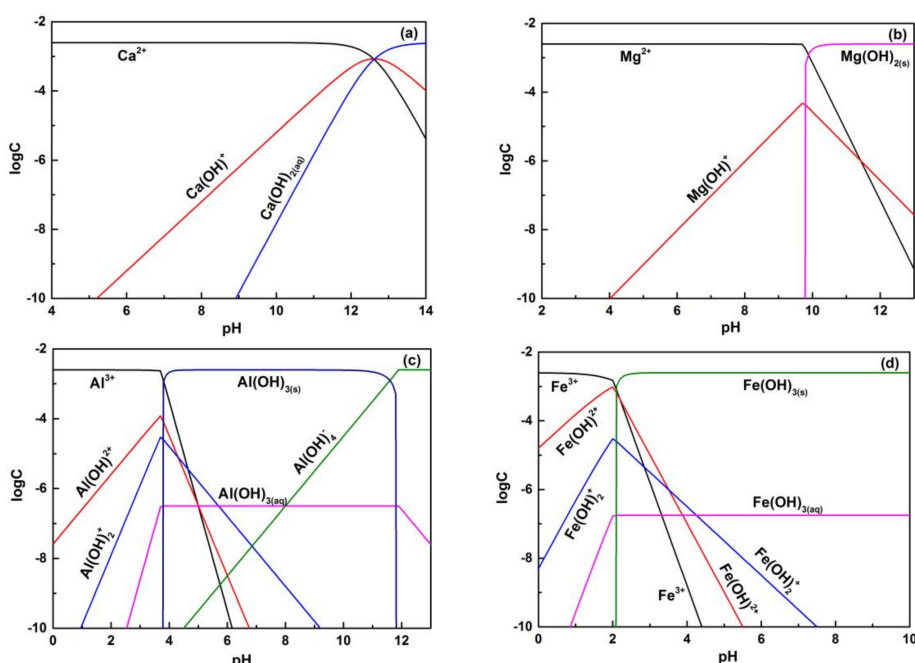


**Figure 5.** The logC–pH diagram for hydrolysis species of (a)  $Ca^{2+}$ ; (b)  $Mg^{2+}$ ; (c)  $Al^{3+}$ ; (d)  $Fe^{3+}$  with the initial ionic concentration of  $2.5 \times 10^{-3}$  M.

As the dominant species around the neutral pH, divalent calcium, and magnesium ions were specifically adsorbed on the mineral surface in apatite and dolomite flotation. It can be speculated that the adsorption of  $\text{Ca}^{2+}$  or  $\text{Mg}^{2+}$  on the apatite surface can increase the active sites which react with the carboxylate ion of fatty acid soap, contributing to the improvement of apatite floatability. The high recovery of dolomite was mainly attributed to the relatively high concentration of cations in the surface lattice [24], thus a low concentration of  $\text{Ca}^{2+}$  and  $\text{Mg}^{2+}$  exhibited a negligible influence on the flotation performance of dolomite. However, in the case of high concentration, the extra divalent metal ions in the bulk would react with fatty acid soap, reducing the amount available for dolomite collection [12].

The activation of quartz by metal ions was attributed to the chemisorption of hydroxides on the mineral surface. Han et al. [25] investigated the activation of quartz as a function of pH in the presence of  $10^{-4}$  M metal ions and sulfonate collector, and the first hydroxy species were found to be responsible for the increase of quartz recovery under a particular pH. As shown in Figure 4a, the maximum quartz recovery was obtained at a pH of about 12.2 in the presence of  $\text{Ca}^{2+}$  and 10.0 for  $\text{Mg}^{2+}$ . The species distribution diagrams of  $\text{Ca}^{2+}$  and  $\text{Mg}^{2+}$  indicate that  $\text{Ca}(\text{OH})^+$  and  $\text{Mg}(\text{OH})^+$  increase to the maximum at pH of 12.4 and 9.8, respectively. Furthermore, it can be seen that the maximum recovery of quartz coincided with the conditions for the maximum concentration of the first hydroxy species of calcium and magnesium. Meanwhile, the logC–pH diagram showed that it was the precipitate of  $\text{Al}(\text{OH})_3$  and  $\text{Fe}(\text{OH})_3$ , instead of free metal ions, that was the major species in the pH range 4.0–10.0 and is likely the reason why the activation of  $\text{Al}^{3+}$  and  $\text{Fe}^{3+}$  on quartz was lower than that of  $\text{Ca}^{2+}$  and  $\text{Mg}^{2+}$ .

### 3.3. Zeta Potentials of Pure Minerals in the Presence of Calcium Ions

As the precipitations of  $\text{Mg}(\text{OH})_2$ ,  $\text{Al}(\text{OH})_3$ , and  $\text{Fe}(\text{OH})_3$  were generated in solution under certain pH conditions, the accuracy of potential measurements of pure minerals would be affected by the coating of these metal hydroxides on the mineral surface. Hence, the effect of calcium ions on the zeta potential of minerals was studied. Previous studies were focused separately on the zeta potential measurements of apatite [26,27], dolomite [24,28], and quartz [29] in the presence of calcium ions. In fact, the zeta potentials varied due to different ionic strength, experimental apparatus, sample preparation process, etc. The effects of calcium ions on the zeta potentials of apatite, dolomite, and quartz as a function of pH were of great necessity to investigate simultaneously in this study. The results are shown in Figures 6–8.

It can be seen from Figure 6 that the isoelectric point (IEP) of apatite was about 3.4 in distilled water, which was almost in agreement with the value of pH = 3 obtained by Hu and Xu [30]. The IEP values shift to 4.3 and 9.6 in the presence of calcium ions at concentrations of  $2.5 \times 10^{-4}$  M and  $2.5 \times 10^{-3}$  M, respectively. Amankonah and Somasundaran [26] identified that the shifts could be attributed to surface reaction and/or bulk precipitation. Besides, the apatite surface was more positively charged with the increase of calcium ion concentration, and a relatively great variation of zeta potential was observed at pH 4–10 while small changes were shown above pH 11 in the presence of  $\text{Ca}^{2+}$ . This indicates that calcium ions were mainly and specifically adsorbed on the apatite surface in the form of divalent cations at a particular pH range (pH < 10).

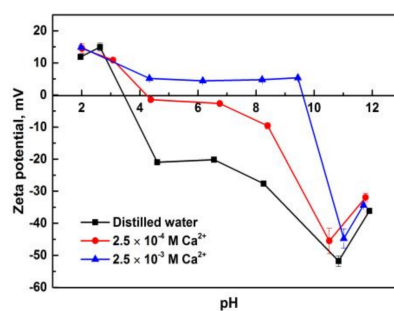


**Figure 6.** Zeta potential of apatite as a function of pH in the absence and presence of calcium ions.

Due to the dissolution of dolomite in acid conditions, the measurement was conducted with a pH above 9, and the results are plotted in Figure 7. Though the IEP of dolomite without  $\text{Ca}^{2+}$  has not been observed over the entire pH studied, it can be seen that the IEP value shifted from 10 to 11.25, with the addition of  $\text{Ca}^{2+}$  at concentrations from  $2.5 \times 10^{-4}$  to  $2.5 \times 10^{-3}$  M. The IEP was reported at pH 6.0 based on the species distribution of dolomite [31], and pH 6.2 as obtained by measurement [32].

In contrast to the zeta potential of  $-20.93$  mV charged on the surface of apatite at pH 4.6 and much more negative above pH 10.8 in the absence of calcium ions, it is interesting to note that the minimum value of the zeta potential of dolomite was just  $-17.47$  mV at pH 11.7. Therefore, it can be inferred that there is a higher concentration of metal cations on the surface of dolomite than that of apatite, which is likely responsible for their different flotation behaviors in the anionic flotation.

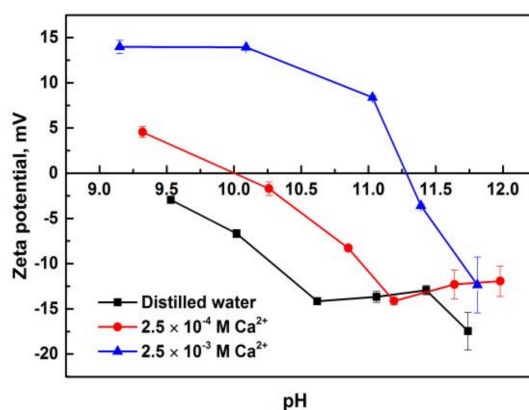


Figure 7. Zeta potential of dolomite as a function of pH in the absence and presence of calcium ions.

Figure 8 shows the zeta potential of quartz as a function of pH in the absence and presence of calcium ions. The IEP of quartz in distilled water was observed around pH = 2, which was in good agreement with results reported by other researchers [33–35]. It can be seen that the IEP values did not change with the increase of calcium ion concentration, but the quartz surface was less negatively charged in the presence of  $\text{Ca}^{2+}$  above pH 3.4. Meanwhile, an obvious variation of zeta potential was observed under the pH conditions from 8 to 12.

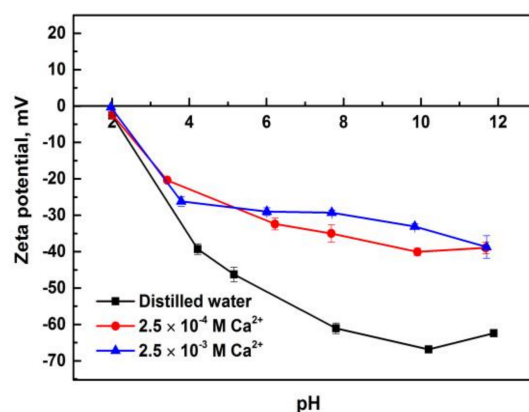


Figure 8. Zeta potential of quartz as a function of pH in the absence and presence of calcium ions.

According to the species distribution diagram shown in Figure 5, calcium ions existed as free ions below pH 12, while the concentration of  $\text{Ca}(\text{OH})^+$  was up to  $6.3 \times 10^{-7}$  M at pH 9, and at a maximum of  $8.5 \times 10^{-4}$  M at pH 12.6. There was no flotation response of quartz observed in Figure 4a under the pH of 9, even though the zeta potential became less negative in the presence of calcium ions. This was

caused by the compression of the electric double layer. In this case, the  $\text{Ca}^{2+}$  ions were mobile in the diffuse layer and not adsorbed in the Stern plane and fixed on the solid surfaces [23]. Therefore, they could not help quartz to adsorb carboxylates. Hence the activation mechanism of quartz was likely related to the chemisorbed  $\text{Ca}(\text{OH})^+$  on the surface or surface precipitation.

### 3.4. XPS Analyses and High-Resolution Spectra of Pure Minerals

To further directly investigate the effect of  $\text{Ca}^{2+}$  on the flotation behaviors of different minerals, the atomic percent of elements for the surfaces of apatite, dolomite, and quartz in various conditions was determined by XPS [36]. The results presented in Tables 2 and 3 indicated that the atomic percent of calcium slightly increased when apatite and dolomite were conditioned in a  $2.5 \times 10^{-3}$  M  $\text{Ca}^{2+}$  solution at neutral pH. After the flotation, using cottonseed oil soap as a collector, the carbon concentration apparently increased with a decrease of the oxygen and calcium concentrations, suggesting the adsorption of collector on the mineral surfaces. Moreover, the magnitude of adsorption was enhanced in the presence of calcium ions.

As shown in Table 4, the increase of calcium concentrations and the corresponding decrease of silicon concentrations were observed for quartz surfaces in the presence of calcium ions. After the interaction between activated quartz and collector, the carbon concentration drastically increased from 14.50% to 53.96%, indicating the significant adsorption of collector on the quartz surfaces. Additionally, a further increase of the calcium concentration proved that the collector reacted with free calcium ions in the pulp and precipitate on quartz surfaces.

**Table 2.** Atomic percent of elements for apatite surfaces in various conditions (pH = 7.0).

Sample	Elements (Atomic %)				
	O1s	C1s	Ca2p	P2p	F1s
Apatite	45.89	24.95	15.30	10.13	3.73
Apatite + $\text{Ca}^{2+}$	45.01	25.43	15.82	9.90	3.84
Apatite + collector	41.19	33.35	13.21	9.65	2.60
Apatite + $\text{Ca}^{2+}$ + collector	38.62	36.07	13.22	8.89	3.20

**Table 3.** Atomic percent of elements for dolomite surfaces in various conditions (pH = 7.0).

Sample	Elements (Atomic %)			
	O1s	C1s	Ca2p	Mg1s
Dolomite	51.66	34.14	9.26	4.94
Dolomite + $\text{Ca}^{2+}$	50.27	36.45	9.48	3.80
Dolomite + collector	44.87	43.51	8.55	3.07
Dolomite + $\text{Ca}^{2+}$ + collector	43.64	45.29	8.50	2.57

**Table 4.** Atomic percent of elements for quartz surfaces in various conditions (pH = 11.0).

Sample	Elements (Atomic %)			
	O1s	C1s	Ca2p	Si2p
quartz	55.04	14.16	-	30.80
quartz + $\text{Ca}^{2+}$	57.78	14.50	0.17	27.55
quartz + $\text{Ca}^{2+}$ + collector	29.38	53.96	1.48	15.18

The C1s spectra of samples shown in Figure 9 can be fitted with four component binding energies of C1s at around 284.87 eV, 285.85 eV, 288.65 eV and 289.85 eV that originated from the carbon atoms in functional groups of C–C/C–H, C–O, C=O and O–C=O, respectively [36–38]. In the absence of

collector in solution, the binding energy at around 284.80 eV for apatite, dolomite, and quartz can be attributed to adventitious carbon contamination.

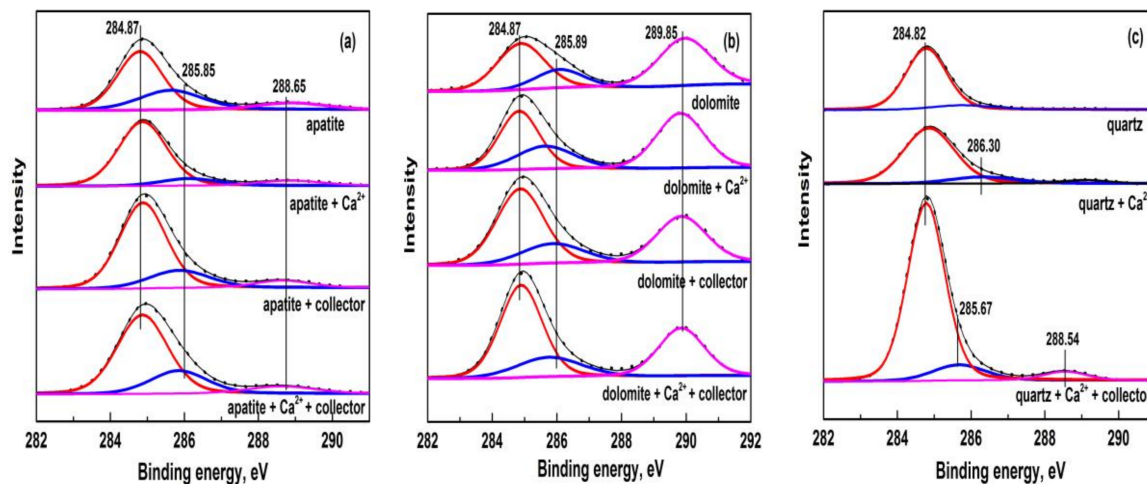


**Figure 9.** High resolution C1s spectra of (a) apatite; (b) dolomite; (c) quartz in the absence and presence of  $2.5 \times 10^{-3}$  M  $\text{Ca}^{2+}$  and 60 mg/L cottonseed oil soap.

According to the results shown in Figure 9a and Table S1, calcium ions can enhance the intensity and area of binding energy positioned at 285.85 eV and 288.65 eV for the apatite, suggesting an increased adsorption of C–O and C=O sourced from fatty acid soap. However, there were no apparent changes to be observed from the C1s spectra of dolomite in the absence and presence of  $\text{Ca}^{2+}$  using anionic collector (Figure 9b, Table S2). The intensity and area of binding energy at 284.82 eV exhibited a significant increase on the surface of quartz being floated, and that of higher binding energies at 285.67 eV and 288.54 eV concurrently increased (Figure 9c, Table S3). On the other hand, the peak was observed to shift towards the lower binding energy from 286.30 to 285.67 eV in the presence of calcium ions and collector, indicating the chemisorption of reagent on the activated quartz surface [39]. These results can be well explained by the different effects of  $\text{Ca}^{2+}$  on the flotation behavior of apatite, dolomite and quartz at a concentration of  $2.5 \times 10^{-3}$  M.

#### 4. Conclusions

1. The flotation behaviors of apatite, dolomite, and quartz, in the presence of metal ions, were investigated through micro-flotation tests. The beneficial effect of  $\text{Ca}^{2+}$  and  $\text{Mg}^{2+}$  with an appropriate concentration on anionic flotation of apatite was confirmed, and was proved negligible on that of dolomite. Excessive amounts of  $\text{Ca}^{2+}$  can reduce the floatability of apatite and dolomite at neutral pH. Both  $\text{Al}^{3+}$  and  $\text{Fe}^{3+}$  exhibited a depression effect on these calcium-bearing minerals. Quartz can be activated by metal ions, and its floatability varied under different pH conditions and metal ion species.
2. Solution chemistry and zeta potential measurement indicate that the influence of metal ions on the flotation of apatite, dolomite and quartz are attributed to the adsorption of various hydrolysis species of metal ions on the mineral surfaces. It was inferred that  $\text{Ca}^{2+}$  and  $\text{Mg}^{2+}$  were mainly adsorbed on the apatite and dolomite surface in the form of divalent ions while  $\text{Ca}(\text{OH})^+$  and  $\text{Mg}(\text{OH})^+$  were responsible for the activation of quartz.
3. Various adsorption characteristics of collector on apatite, dolomite, and quartz surfaces in the absence and presence of calcium ions were revealed by XPS analyses, which was in agreement with the flotation results of these minerals under the same ionic concentration.

**Supplementary Materials:** The following are available online at <http://www.mdpi.com/2075-163X/8/4/141/s1>, Table S1: Parameters of C1s on apatite surface treated with various conditions; Table S2: Parameters of C1s on dolomite surface treated with various conditions; Table S3: Parameters of C1s on quartz surface treated with various conditions.

**Acknowledgments:** The authors would like to acknowledge the financial support from National Science Foundation of China (51404171) and Hubei Technical Innovation Project (2017ACA187).

**Author Contributions:** R.C., Z.Z. and H.L. conceived and designed the experiments; Y.R. performed the experiments; R.C. and Y.R. analyzed the data; C.X. and F.Z. contributed reagents/materials/analysis tools; Y.R. wrote the paper.

**Conflicts of Interest:** The authors declare no conflict of interest.

## References

1. Ejtemaei, M.; Irannajad, M.; Gharabaghi, M. Role of dissolved mineral species in selective flotation of smithsonite from quartz using oleate as collector. *Int. J. Miner. Process.* **2012**, *114–117*, 40–47. [[CrossRef](#)]
2. Bulut, G.; Yenial, Ü. Effects of major ions in recycled water on sulfide minerals flotation. *Miner. Metall. Process.* **2016**, *33*, 137–143. [[CrossRef](#)]
3. Liu, W.; Zhang, S.; Wang, W.; Zhang, J.; Yan, W.; Deng, J.; Feng, Q.; Huang, Y. The effects of Ca(II) and Mg(II) ions on the flotation of spodumene using NaOL. *Miner. Eng.* **2015**, *79*, 40–46. [[CrossRef](#)]
4. Jeldres, R.I.; Arancibia-Bravo, M.P.; Reyes, A.; Aguirre, C.E.; Cortes, L.; Cisternas, L.A. The impact of seawater with calcium and magnesium removal for the flotation of copper-molybdenum sulphide ores. *Miner. Eng.* **2017**, *109*, 10–13. [[CrossRef](#)]
5. Nanthakumar, B.; Grimm, D.; Pawlik, M. Anionic flotation of high-iron phosphate ores—Control of process water chemistry and depression of iron minerals by starch and guar gum. *Int. J. Miner. Process.* **2009**, *92*, 49–57. [[CrossRef](#)]
6. Choi, J.; Choi, S.Q.; Park, K.; Han, Y.; Kim, H. Flotation behavior of malachite in mono- and di-valent salt solutions using sodium oleate as a collector. *Int. J. Miner. Process.* **2016**, *146*, 38–45. [[CrossRef](#)]
7. Liu, D.; Somasundaran, P.; Vasudevan, T.V.; Harris, C.C. Role of pH and dissolved mineral species in Pittsburgh No. 8 coal flotation system—1. Floatability of coal. *Int. J. Miner. Process.* **1994**, *41*, 201–214. [[CrossRef](#)]
8. Huang, P.; Fuerstenau, D.W. The effect of the adsorption of lead and cadmium ions on the interfacial behavior of quartz and talc. *Colloids Surf. A* **2001**, *177*, 147–156. [[CrossRef](#)]
9. Scott, J.L.; Smith, R.W. Calcium ion effects in amine flotation of quartz and magnetite. *Miner. Eng.* **1993**, *6*, 1245–1255. [[CrossRef](#)]
10. Abouzeid, A.-Z.M. Physical and thermal treatment of phosphate ores—An overview. *Int. J. Miner. Process.* **2008**, *85*, 66. [[CrossRef](#)]
11. Sis, H.; Chander, S. Adsorption and contact angle of single and binary mixtures of surfactants on apatite. *Miner. Eng.* **2003**, *16*, 841–847. [[CrossRef](#)]
12. Santos, M.A.; Santana, R.C.; Capponi, F.; Ataíde, C.H.; Barrozo, M.A.S. Effect of ionic species on the performance of apatite flotation. *Sep. Purif. Technol.* **2010**, *76*, 15–20. [[CrossRef](#)]
13. Al-Thyabat, S.; Al-Zoubi, H. Purification of phosphate beneficiation wastewater: Separation of phosphate from Eshydia Mine (Jordan) by column-DAF flotation process. *Int. J. Miner. Process.* **2012**, *110–111*, 21–23. [[CrossRef](#)]
14. Elgillani, D.A.; Abuzeid, A.-Z.M. Flotation of carbonates from phosphate ores in acidic media. *Int. J. Miner. Process.* **1993**, *38*, 239–246. [[CrossRef](#)]
15. Al-Wakeel, M.I.; Lin, C.L.; Miller, J.D. Significance of liberation characteristics in the fatty acid flotation of Florida phosphate rock. *Miner. Eng.* **2009**, *22*, 244–253. [[CrossRef](#)]
16. Ruan, Y.; Zhang, Z.; Luo, H.; Xiao, C.; Zhou, F.; Chi, R. Ambient temperature flotation of sedimentary phosphate ore using cottonseed oil as a collector. *Minerals* **2017**, *7*, 65. [[CrossRef](#)]
17. Horta, D.; Monte, M.B.M.; Leal Filho, L.S. The effect of dissolution kinetics on flotation response of apatite with sodium oleate. *Int. J. Miner. Process.* **2016**, *146*, 97–104. [[CrossRef](#)]
18. Tohry, A.; Dehghani, A. Effect of sodium silicate on the reverse anionic flotation of a siliceous-phosphorus iron ore. *Sep. Purif. Technol.* **2016**, *164*, 31–32. [[CrossRef](#)]

19. Zhang, G.F.; Feng, Y.; Zhu, Y.G.; Tang, P.H. Influence of  $\text{Ca}^{2+}$ ,  $\text{Mg}^{2+}$  on apatite and dolomite flotation. *Ind. Miner. Process.* **2011**, *7*, 1–4. (In Chinese)
20. Araújo, A.C.A.; Lima, R.M.F. Influence of cations  $\text{Ca}^{2+}$ ,  $\text{Mg}^{2+}$  and  $\text{Zn}^{2+}$  on the flotation and surface charge of smithsonite and dolomite with sodium oleate and sodium silicate. *Int. J. Miner. Process.* **2017**, *167*, 35–41. [[CrossRef](#)]
21. Ananthapadmanabhan, K.P.; Somasundaran, P. Surface precipitation of inorganics and surfactants and its role in adsorption and flotation. *Colloids Surf.* **1985**, *13*, 151–167. [[CrossRef](#)]
22. Somasundaran, P.; Wang, D.Z. *Solution Chemistry: Minerals and Reagents*, 1st ed.; Elsevier: Amsterdam, The Netherlands, 2006; pp. 45–57.
23. Fuerstenau, M.C.; Lopez-Valdivieso, A.; Fuerstenau, D.W. Role of hydrolyzed cations in the natural hydrophobicity of talc. *Int. J. Miner. Process.* **1988**, *23*, 161–170. [[CrossRef](#)]
24. Kasha, A.; Al-Hashim, H.; Abdallah, W.; Taherian, R.; Sauerer, B. Effect of  $\text{Ca}^{2+}$ ,  $\text{Mg}^{2+}$  and  $\text{SO}_4^{2-}$  ions on the zeta potential of calcite and dolomite particles aged with stearic acid. *Colloids Surf. A* **2015**, *482*, 293–298. [[CrossRef](#)]
25. Han, K.N.; Healy, T.W.; Fuerstenau, D.W. The mechanism of adsorption of fatty acids and other surfactants at the oxide-water interface. *J. Colloid Interface Sci.* **1973**, *44*, 407. [[CrossRef](#)]
26. Amankonah, J.O.; Somasundaran, P. Effects of dissolved mineral species on the electrokinetic behavior of calcite and apatite. *Colloids Surf.* **1985**, *15*, 335–353. [[CrossRef](#)]
27. Vucinic, D.R.; Radulovic, D.S.; Deusic, S.D. Electrokinetic properties of hydroxyapatite under flotation conditions. *J. Colloid Interface Sci.* **2010**, *343*, 239–245. [[CrossRef](#)] [[PubMed](#)]
28. Pokrovsky, O.S.; Schott, J.; Thomas, F. Dolomite surface speciation and reactivity in aquatic systems. *Geochim. Cosmochim. Acta* **1999**, *63*, 3137. [[CrossRef](#)]
29. Kou, J.; Xu, S.; Sun, T.; Guo, Y.; Wang, C. A study of sodium oleate adsorption on  $\text{Ca}^{2+}$  activated quartz surface using quartz crystal microbalance with dissipation. *Int. J. Miner. Process.* **2016**, *154*, 26–27. [[CrossRef](#)]
30. Hu, Y.; Xu, Z. Interactions of amphoteric amino phosphoric acid with calcium-containing minerals and selective flotation. *Int. J. Miner. Process.* **2003**, *72*, 91. [[CrossRef](#)]
31. Chen, G.; Tao, D. Effect of solution chemistry on flotability of magnesite and dolomite. *Int. J. Miner. Process.* **2004**, *74*, 354–356. [[CrossRef](#)]
32. Gence, N.; Ozbay, N. pH dependence of electrokinetic behavior of dolomite and magnesite in aqueous electrolyte solutions. *Appl. Surf. Sci.* **2006**, *252*, 8059–8060. [[CrossRef](#)]
33. Vidyadhar, A.; Rao, K.H. Adsorption mechanism of mixed cationic/anionic collectors in feldspar-quartz flotation system. *J. Colloid Interface Sci.* **2007**, *306*, 198. [[CrossRef](#)] [[PubMed](#)]
34. Yao, J.; Yin, W.; Gong, E. Depressing effect of fine hydrophilic particles on magnesite reverse flotation. *Int. J. Miner. Process.* **2016**, *149*, 88. [[CrossRef](#)]
35. Liu, W.; Liu, W.; Wang, X.; Wei, D.; Wang, B. Utilization of novel surfactant N-dodecyl-isopropanolamine as collector for efficient separation of quartz from hematite. *Sep. Purif. Technol.* **2016**, *162*, 192. [[CrossRef](#)]
36. Buckley, A.N. A survey of the application of X-ray photoelectron spectroscopy to flotation research. *Colloids Surf. A* **1994**, *93*, 168–169. [[CrossRef](#)]
37. Sahoo, H.; Rath, S.S.; Das, B.; Mishra, B.K. Flotation of quartz using ionic liquid collectors with different functional groups and varying chain lengths. *Miner. Eng.* **2016**, *95*, 108–110. [[CrossRef](#)]
38. Gouzman, I.; Dubey, M.; Carolus, M.D.; Schwartz, J.; Bernasek, S.L. Monolayer vs. multilayer self-assembled alkylphosphonate films: X-ray photoelectron spectroscopy studies. *Surf. Sci.* **2006**, *600*, 776–777. [[CrossRef](#)]
39. Chen, P.; Zhai, J.; Sun, W.; Hu, Y.; Yin, Z. The activation mechanism of lead ions in the flotation of ilmenite using sodium oleate as a collector. *Miner. Eng.* **2017**, *111*, 100–107. [[CrossRef](#)]

